Analysis of *in-patient* evolution of *Escherichia coli* reveals potential links to relapse of bone and joint infections

Stanislas THIRIET-RUPERT[a], Jérôme JOSSE[b], David PEREZ-PASCUAL[a], Jason TASSE[b], Camille ANDRE[b], Léila ABAD[b], David LEBEAUX[a,c,d], Jean-Marc GHIGO[a], Frédéric LAURENT[b] and Christophe BELOIN[a]#

[a] *Institut Pasteur, Université de Paris-Cité, CNRS UMR6047, Genetics of Biofilms Laboratory F-75015 Paris, France.*

[b] *CIRI, Centre International de Recherche en Infectiologie, Inserm, U1111, Université Claude Bernard Lyon 1, CNRS, UMR5308, École Normale Supérieure de Lyon, 69007, France.*

[c] *Département de Maladies Infectieuses et Tropicales, AP-HP, Hôpital Saint-Louis, Lariboisière, F-75010 Paris, France.*

[d] *FHU PROTHEE*

Running Head: in-patient evolution of *E. coli* in BJIs

#Adress correspondence to christophe.beloin@pasteur.fr (ORCID: 0000-0002-0344-3443)

Author contributions: C.B., S.T.-R., F.L., J.J. designed the experiments. S.T.-R., J.J., D.P.-P., J.T., C.A., and L.A. performed the experiments. C.B., S.T.-R., F.L., J.J., D.L. and J.-M.G. analyzed data. S.T.-R., C.B., D.P.-P. and J.J. wrote the manuscript with significant help of D.L., F.L. and J.-M.G..

Abstract

Bone and joint infections (BJIs) are difficult to treat and affect a growing number of patients, in which relapses are observed in 10-20% of the case. These relapses, which call for prolonged antibiotic treatment and increase the risk of emergence of resistance, may originate from ill understood adaptation of the pathogen to the host. Here, we studied three pairs of *Escherichia coli* strains corresponding to three cases of BJIs and their relapse to better understand in-patient adaptation.

Whole genome comparison presented evidence for positive selection with prevalence of non-synonymous and loss of function mutations. Phenotypic characterization showed that biofilm formation capacity was not modified, contrary to what is usually described in such relapse cases. Although virulence was not modified, we identified the loss of two virulence factors (namely an AFA afimbrial adhesin and a YadA-like adhesin) contributing to immune system evasion in one of the studied relapse strain. Other selected strategies likely helped the relapse strains to outcompete competitors through global growth optimization and colicin production. This work highlights the variety of strategies allowing in-patient adaptation in BJIs.

Keywords: BJI, adaptation, relapse, *Escherichia coli,* in patient evolution

50 ## Introduction **(298 words)**

51 Bone and joint infections (BJIs), including prosthetic joint infections (PJI), are severe
52 and difficult to treat infections affecting a growing number of patients, and showing 10 to 20%
53 of relapse (1–6). Although staphylococci are responsible for more than 50% of all BJI, 20% of
54 them are caused by *Enterobacterales*, especially in the case of early and late acute infections
55 (7), whereas *Pseudomonas aeruginosa* infections are associated with particularly difficult to
56 treat BJI (6). These data therefore support the need to study BJI caused by both Gram-positive
57 and Gram-negative bacteria and for a better understanding of the *in vivo* adaptation leading to
58 relapses.
59
60 During host colonization, pathogenic bacteria must face different selective stresses
61 including host defenses and interactions with the endogenous microbiota or other co-infecting
62 bacteria. This competition could involve toxin production (8, 9) and other adaptive strategies
63 to access resources (10) and evade the host immune system (11, 12), eventually leading to a
64 decrease virulence accounting for bacterial persistence in the host.
65
66 The genetic modifications underlying these adaptations are in general quite restricted upon
67 natural host purifying selection (13, 14). In some extreme cases, mutator genotypes can evolve,
68 thus facilitating within-host adaptation (15, 16). Extensive genome reductions and
69 rearrangements (17–19) are also observed leading to the loss of non-essential genes in the host
70 environment. However, there is an increasing body of evidence that these gene losses could
71 also fuel adaptative evolution and microbial adaptation within patient is currently under intense
72 scrutiny (20, 21). However, acquiring longitudinal samples and studying pathogens adaptation
73 from the same patient in the context of infection relapses is difficult (22). In this study, we
74 analysed three pairs of *E. coli* strains isolated from initial and recurrent BJIs in 3 patients to

75 investigate how *in-patient* evolution occurred in these situations and provide insights on the
76 potential mechanisms involved in infection relapse.
77
78
79 # Methods
80
81 **Selection of clinical strains**
82 Initial / Relapse pairs of clinical *E. coli* strains used in this study were selected among the
83 routine collections of the Bacteriology Department of Hôpital de la Croix-Rousse, Hospices
84 Civils de Lyon and the Bacteriology laboratory at Cerballiance (Lyon, France). The first search
85 criterion corresponded to collect *E. coli* strains isolated from BJI from 2017 to 2020. Then,
86 initial/relapse pairs were formed when *E. coli* strain was isolated in two different samples at
87 two different times in the same patient (initial and relapse) and at the same site of infection.
88 Strain characteristics are available in Table 1. Antimicrobial susceptibility tests were performed
89 by using the disc diffusion method (Supplementary Table 1).
90
91 **Bacterial strains and growth conditions**
92 Bacterial strains used in this study are listed in Supplementary Table 2. Bacteria were grown in
93 Miller's Lysogeny Broth (LB) (Corning) or M63B1 minimum medium supplemented with
94 appropriate antibiotic and carbon source as specified. Liquid cultures were incubated at 37°C
95 or 30°C with 180rpm shaking. Solid cultures were done on LB with 1.5% agar supplemented
96 with the appropriate antibiotics. Chemicals and media were purchased from Sigma-Aldrich.
97
98 **Strain construction**

99 Insertion of a Zeo-GFP and Zeo-mars genetic cassettes at the permissive lambda *att* attachment
100 site as well as the deletion of *fliC* in I1 and R1 strains and the deletion of two adhesin coding
101 genes in I2 strain were done using pKOBApra plasmid (23) and lambda-red recombination.
102 Primers used for genetic constructions are listed in Supplementary Table 3.
103
104 **RDAR morphotypes on congo red plates**
105 Two microliters of an overnight culture grown at 37°C in LB medium under shaking (with
106 appropriate antibiotics when needed) was spotted onto LB plates (without NaCl) containing
107 0.004% Congo Red and 0.002% brilliant blue. The spotted drops were allowed to dry, and the
108 plates were incubated for 24 and 48 hours at 30 or 37°C.
109
110 **Auto-aggregation curves**
111 Cultures were grown as described above, and 1mL aliquots were diluted to an OD_{600}=3 in spent
112 medium in order to prevent growth during experiment. Once diluted, all the tubes were vortexed
113 and an aliquot of 50µL was removed, 1cm below the top of the culture, and diluted with 50µL
114 of LB prior to OD_{600} measurement. The bacteria were then left to aggregate at RT for 6 hours,
115 while repeating the measurement of OD_{600} 1 cm below the top of the culture every hour.
116
117 **Biofilm microtiter plate CV assay**
118 Bacteria were grown overnight and diluted to an OD_{600}=0.05 and 100µL were inoculated in
119 technical triplicates in either a polystyrene Greiner 96-well plate or a polyvinyl chloride (PVC)
120 round bottom 96-well plates (Corning). For each experiment a second identical plate was
121 inoculated to assess growth. After 24 hours at 37°C, one plate was resuspended to measure the
122 OD_{600}. In the other plate, non-attached bacteria were washed away by flicking and wells were
123 washed twice with water. Biofilms were stained with 125µL of crystal violet 1% (V5265;

124 Sigma-Aldrich) for 15 minutes. Crystal violet was then removed by flicking and washed three
125 times with water and plates were allowed to dry up. Biofilms were then resuspended using a
126 solution of acetone:ethanol 1:5 mix, and OD_{575} was measured using Tecan Infinite-M200-Pro
127 spectrophotometer. To account for potential differences in growth capacities, the OD_{575} values
128 were normalized by OD_{600}.
129
130 **CFU counting on biomaterials**
131 The biofilm forming capacity was assessed on different orthopaedic biomaterials [stainless steel
132 (AISI 316L), titanium (TA6V), medical grade silicone and ultra-high molecular weight
133 polyethylene (UHMWPE)]. Uniform cylindrical pegs of orthopaedic biomaterial were
134 manufactured by a supplier of medical and surgical orthopaedics equipment (Groupe Lépine,
135 Genay, France) under the same conditions of manufacture of orthopaedic biomaterial and
136 sterilized by gamma rays. Biomaterial pegs were fixed into the lid of 24-well flat-bottom cell
137 culture plates (Corning Inc., Corning, NY, USA). Bacterial biofilms were formed by immersing
138 the lid-containing pegs into 2mL of cultures at OD_{600}=0.05 and incubated in LB for 24 hours at
139 37°C in humid atmosphere. After 3 rinsing steps in PBS, the pegs were dropped in a Falcon
140 tube containing 5mL of PBS for biofilm disruption using sonication for 5 minutes
141 (BACTOSONIC 14.2, BANDELIN, Berlin, Germany). Then, viable cell count was determined
142 by serial dilution and plating.
143
144 **Bacterial adhesion to MG63 human osteoblastic cells**
145 The osteoblastic cell line MG63 (LGC standards, Molsheim, France) was used to test bacterial
146 adhesion. Cells were cultured in 75cm² flasks (T75, BD Falcon, Le Pont de Claix, France) at
147 37°C under 5% CO_2, in a culture medium composed of DMEM (Dulbecco's Modified Eagle
148 Medium containing D-glucose, L-glutamine, pyruvate) supplemented with 10% fetal calf serum

149 (FCS), penicillin (100µg/mL) and streptomycin (100µg/mL), all from Gibco (Paisley, UK).
150 Cells were passaged once a week and used until passage 25 at the most. The day before the
151 infection, MG63 cells were seeded at 100,000 cells per well in a 24-well plate and the different
152 bacterial strains were inoculated in LB. The day of the infection, overnight bacterial cultures
153 were centrifugated, resuspended and adjusted in DMEM + 10% FCS to reach a MOI
154 (multiplicity of infection) of 100:1 and added to cell culture. After 2 hours of infection, cells
155 were washed twice with PBS and incubated and lysed by osmotic shock in sterile water and
156 lysates were plated on tryptone soy agar plates (Biomérieux) using the Easy Spiral® automaton
157 (Interscience, Saint-Nom-la-Bretèche, France). CFU were counted after 18 hours of incubation
158 at 37°C and results were presented as CFU for 100,000 cells.
159
160 **Growth capacity**
161 An overnight culture of each strain was diluted to OD_{600} of 0.05 in appropriate medium. One
162 hundred and fifty µL aliquots were inoculated in a 96-well plate. The plates were then incubated
163 in a TECAN Infinite M200 Pro spectrophotometer (Männedorf, Switzerland) for 18 hours at
164 37°C with shaking of 2mm amplitude. The absorbance of each culture at 600 nm was measured
165 every 15 minutes. Growth curve of each strain was measured using 3 biological replicates.
166 The R package GrowthCurver (24) was used to infer growth-related parameters for all strains
167 based on the growth curves.
168
169 **Cytotoxicity on HeLa cells**
170 The cytotoxic activity on Hela cells of each bacterial strain was analyzed using the CellTiter-
171 Blue® Cell Viability Assay (Promega) following manufacturer instructions. HeLa cells were
172 cultured in complete DMEM (Life Technologies) supplemented with 10% FCS, 100µg/mL
173 penicillin/streptomycin, and 10mM L-glutamine at 37C in the presence of 5% CO_2. For

174 infection assay, the HeLa cells were incubated in 96-well plates to reach a density of 10^5 cells.
175 Each bacterial strain was grown overnight in LB as described above and then washed twice in
176 PBS, to finally adjust the bacterial density to 10^7 CFU/ml. These bacterial suspensions were
177 used to infect HeLa cells by adding 100 µl of each to the wells (MOI of 1:100). The plates were
178 incubated at 37C in the presence of 5% CO_2 for 2 hours. Non-infected cells and the *E. coli* K12
179 MG1655 strain were used as negative controls. At the end of the incubation time, the wells
180 were washed twice with PBS to remove the bacteria. Then, 100 µl of PBS and 20 µl of CellTiter
181 Blue solution were added to each well and incubated for 2 hours at 37C and 5% CO_2. The cell
182 viability was measured by recording the fluorescence at 560/590 nm using a Tecan Infinite-
183 M200-Pro spectrophotometer.
184
185 **Hemolysis capacity**
186 The hemolytic activity of each strain was assessed by mixing defibrinated horse blood
187 (bioMerieux, Marcy l'Etoile, France) diluted to 10% (v/v) in PBS with a total of 10^8 bacteria
188 in PBS. After 2, 6 and 24 hours of incubation at 37°C with shacking, the non-lysed erythrocytes
189 were pelleted by centrifugation at 1500g for 2 minutes, and the OD_{450} of 150µL of the cell-free
190 supernatants was measured. The hemolytic capacity of each adapted strain was expressed
191 relatively to its ancestral strain.
192
193 **Bacterial survival in human serum**
194 For each strain, 50µL at OD_{600}=0.4 was mixed in a well of a 96-well plat with 50µL of active
195 human serum. The same process was followed for a control with heat-inactivated serum (HIS)
196 (30 minutes at 55°C). The plate was then incubated at 37°C under shaking (450rpm) for 1h30.
197 The content of each well was then serially diluted and plated on LB for CFU count and the

198 survival of each strain was expressed as the ratio between the CFUs in active serum divided by
199 the CFUs in HIS.
200
201 **Zebrafish care and maintenance**
202 Homozygous Tg(*mfap4::mCherryF*) (ump6Tg) (25) Tg(*mpx::GFP*)^{i114} (26) double transgenic
203 fishes were raised in Institut Pasteur zebrafish facility. Eggs were obtained by natural spawning,
204 bleached according to standard protocols, and then kept in Petri dishes containing Volvic spring
205 water and, from 24 hpf onwards, 0.003% 1-phenyl-2-thiourea (PTU) (Sigma-Aldrich) was
206 added to prevent pigmentation. Embryos as well as infected larvae were reared at 28°C. Larvae
207 were anesthetized with 200 µg/mL of buffered tricaine methane sulfonate (MS-222, Sigma-
208 Aldrich) during the injection procedure as well as during *in vivo* imaging and processing for
209 bacterial burden evaluation.
210
211 **Zebrafish infection**
212 Overnight bacterial cultures were centrifuged, washed, and resuspended at the desired
213 concentration in PBS. Anesthetized zebrafish larvae were microinjected intravenously 52–58
214 hours post-fertilization with 1nL of each bacterial suspension at a final concentration of $2x10^3$
215 CFU (27). Infected larvae were transferred into individual wells containing 1mL of mineral
216 Volvic water (Danone, France) and 0.003% 1-phenyl 2-thiourea (used to improve optical
217 transparency in zebrafish) in 24-well plates, incubated at 28°C, and regularly observed under a
218 stereomicroscope. Protocols describing zebrafish maintenance and analysis, see the
219 corresponding supplementary method section.
220
221 **Evaluation of the bacterial burden in infected zebrafish larvae**

222 Infected zebrafish larvae were collected at 0, 24, and 48 hpi and lysed for the evaluation of the
223 bacterial burden as previously described (28). Each larva was placed in an individual 1.5 mL
224 Eppendorf tube and anesthetized with tricaine (200 µg/mL), washed with 1 mL of sterile water,
225 and placed in 150 µL of sterile water. Larvae were then homogenized using a pestle motor
226 mixer (Argos). Each sample was transferred to an individual well of a 96-well plate and 10 X
227 serial dilutions were performed. For CFU enumeration and to assess plasmid stability
228 throughout the infection kinetics, serial dilutions of lysates were plated on MacConkey agar
229 plates supplemented with lactose plates and incubated overnight at 37°C.
230

231 **Visualization of macrophages and neutrophils in infected zebrafish larvae**

232 Visualization of macrophages and neutrophils on living transgenic reporter larvae was
233 performed upon infection as we previously described (29). Briefly, bright field, GFP, and RFP
234 images of whole living anesthetized larvae were taken using a Leica Macrofluo Z16 APOA
235 (zoom 16:1) macroscope equipped with a Leica PlanApo 2.0 X lens, and a Photometrics
236 CoolSNAP *HQ2* camera. Images were captured using the Metavue software version 7.5.6.0
237 (MDS Analytical Technologies). After capture of images, larvae were washed and transferred
238 to a new 24-well plate filled with 1mL of fresh water per well and incubated at 28 °C.
239

240 **Competition assay for biofilm formation**

241 The pair of strains used in competition assay carried two different fluorescent tags and were
242 inoculated in LB medium supplemented with appropriate antibiotic and incubated overnight at
243 37°C under shaking. Cultures were then adjusted to OD_{600} = 0.05 and mixed in 1:1 ratio
244 (verified by FACS). Each competition mix was then inoculated in a PVC plate and incubated
245 at 37°C for 16 hours. The supernatant was removed from each well, the biofilm resuspended in

246 100µL of PBS and the proportion of each strain was assessed by FACS and the relative fitness
247 calculated as follows:

248 $$relative\ fitness = \frac{\left(\frac{Target_{post}}{Target_{pre}}\right)}{\left(\frac{ref_{post}}{ref_{pre}}\right)}$$

249 , where $Target_{pre}$ and $Target_{post}$ are the cell concentrations of the target strain in the mixed
250 culture before and after the overnight incubation, and ref_{pre} and ref_{post} are the cell concentrations
251 of the corresponding reference strain. In order to account for growth differences due to the
252 expression of one or the other fluorescent tag (Supplementary Figure 1), competitions were run
253 with both possible combinations of fluorescent tags. This protocol was used to compete R1 and
254 R3 strains against their respective ancestors. However, because GFP and RFP tags were not
255 expressed in I2 and R2 strains, we used an alternative strategy based on PCR amplification and
256 Sanger sequencing of an SNP locus allowing to distinguish both strains (see Supplementary
257 method section).
258

259 **Competition assay for growth in liquid cultures**

260 The strains were incubated at 37°C in the appropriate medium and adjusted to OD_{600}=0.05. A
261 1:1 ratio mixed culture was verified by FACS and incubated overnight at 37°C with shaking.
262 The concentration of target and reference strains was measured using FACS and relative fitness
263 was calculated as above.
264

265 **Alternative strategy for competition assays of I2 vs R2 strains**

266 Even if we managed to introduce GFP and RFP (mars) tags in I2 and R2 strains, the related
267 proteins were likely not expressed since thefluorescence was impossible to detect.
268 Consequently we used an alternative strategy to assess the proportion of each strain. We took

269 andvantage of the fact that both strains can be differentiated by SNPs. An aliquot of the mixed
270 culture containing 10^7 cells was pelleted and resuspended in 50µL of sterile distiled water and
271 boiled for 10 minutes. Specific primers were then used to amplify a SNP locus in butC gene
272 and Sanger sequence the resulting DNA fragment. Then, using QSVanalyzer (30), we
273 calculated the frequeny of each mutation and used it to compute the relative fitness as above.
274 To assess the accuracy of this strategy, we used strains I1 and R1 taged with different
275 fluorescent marker to compare strains proportions as assessed by FACS and QSVanalyzer and
276 found a very good correspondance between both methods (Supplemenatry Figure S6), therefore
277 validating our alternative approach.
278
279 **Motility assay**
280 Bacterial strains were incubated overnight in LB at the specified temperature with shaking.
281 Then, 2µL of overnight culture was inoculated in swim plates (1% tryptone, 0.25% NaCl,
282 0.25% Eiken agar) for 24 hours at 37°C or 30°C. After incubation, motility was assessed by
283 checking the spread of inoculated bacteria into the motility agar.
284
285 **Overlay assay colicin**
286 I1 and R1 strains were incubated overnight at 37°C with shaking in LB supplemented with 40
287 µg/mL of Mitomycin C to induce colicin production. After incubation an overlay of each strain
288 was realized by pouring 6mL of overnight culture diluted at OD_{600}=0.1 onto a LB agar plate
289 and removing it after 5 minutes. Plates were allowed to dry and a 10µL drop of supernatant
290 from each strain culture filtered using 0.22uM filter was spotted on each overlay. After an
291 additional drying step, the plates were incubated overnight at 37°C and the production of colicin
292 was identified by the presence of an inhibition halo when the filtered supernatant was spotted.

293 LB was spotted as a negative control and filtered supernatant from both strains was also spotted
294 on overlay of each of them to be sur that the growth inhibition halo was not due to the presence
295 of Mitomycin C in the filtered supernatant.
296
297 **Western blot analysis and LPS gel**
298 The heat extracted proteins from 1mL at OD_{600}=1 culture were suspended in 1×Laemmli buffer
299 and incubated for 5 min at 95°C. The protein extracts were run on Mini-PROTEAN TGX Stain-
300 Free precast Gels (BioRad) in 1×TGX buffer and then transferred to nitrocellulose membrane
301 using a Trans-Blot® Turbo Transfer System (BioRad). Blocking was performed in a 5%
302 solution of dry milk and 0.05% Tween 1×PBS (1×PBST) overnight at 4°C with agitation. The
303 membranes were then incubated in 1×PBST with either rabbit anti-flagellin (kindly given by
304 Dr Monica Rolando) or mouse anti-RNAPα (BioLegend #663104) diluted 1/5,000 for 1h at
305 room temperature with agitation. Membranes were washed in 1×PBST and then incubated with
306 the secondary antibody (anti-rabbit or anti-mouse IgG conjugated with horse radish peroxidase
307 at 1:10 000, Promega). The membranes were then revealed using an ECL kit (GE Healthcare)
308 and the iBright™ CL1500 system (Thermofisher).
309 LPS analysis on Mini-PROTEAN TGX Stain-Free precast Gels (BioRad) were realized as in
310 (31).
311
312 **Whole genome sequencing and analysis**
313 Prior to genome extraction, strains were inoculated in LB medium for over-day culture till the
314 OD_{600} reached around 1.0 (ca. $5.0x10^8$ bacteria/mL). The bacterial cells were collected from
315 2mL of the culture and the genomic DNA was extracted using the Wizard Genomic DNA
316 Purification Kit (Promega). Samples were then sent to Novogene Co., Ltd to be sequenced
317 using Illumina NovaSeq 6000. Sequencing reads were pre-processed to remove low-quality or

318 artefactual bases. We used fqCleaner v.0.5.0, a mini workflow implemented in Galaxy (32)
319 (https://galaxy.pasteur.fr/) to process fastq files (quality trimming, duplicate and artifact filters).
320 Draft genomes were de novo assembled using SPAdes version 3.15.0 (33) and annotated using
321 Proka version 1.14.5 (34). Assembly quality and completeness was assessed using BUSCO
322 version v5.4.2 (35). The assembled genomes were used for in silico typing and characterization
323 of each strain using tools available at the Centre of Genomic Epidemiology
324 (http://www.genomicepidemiology.org/): Resfinder (36–38), MLST (38, 39), SerotypeFinder
325 (40), CHtyper (41). Phylogroups were identified in silico using ClermonTyping tool (42). In
326 order to identify contigs corresponding to potential plasmids, each contig was used as a query
327 in a BLASTn search using blast+ version 2.2.31 (38) against the COMPASS database (43).
328 Only hits with 95% identity and 80% coverage of both the query and the hit sequence were
329 kept.
330 Mutations in the adapted strain were identified by using the genome assembly of its ancestral
331 strain as a reference. *breseq* version 0.35.0 (44) with the consensus mode was used with default
332 parameters. The resulting identified mutations were filtered out if they were too close to each
333 other (less than 50bp). These mutations are usually the result of misaligned reads, often due to
334 repetitive regions (45). Because these regions are not 100% identical, they are disturbing the
335 mapping process resulting in false positives. Mutations found in mobile elements were kept if
336 only one copy was present in the genome.
337
338 **Statistical analysis**
339 Figures and statistical tests were performed using either Prism 9.5.1 for Mac OS X (GraphPad
340 Software, Inc.) or Rstudio with R version 4.2.1 using the R package GGplot2 (46).
341
342 **Data availability**

All sequencing reads as well as genome assembly for each strain were deposited in NCBI under the BioProject accession number PRJNA932763. The code used in this study is available at https://github.com/Sthiriet-rupert/BJIs_adaptation.

RESULTS (1151 words)

I- *In-patient* evolved *Escherichia coli* clones showed no antibiotic resistance acquisition but signs of natural selection.

In order to investigate potential cases of *in-patient* adaptation, we obtained three pairs of *E. coli* strains sampled from three patients presenting relapsing BJIs. Each pair is composed of a sample at the time of the initial infection (strains hereafter denominated as I1 to I3 for cases 1 to 3) and a second sample corresponding to the relapse of this infection (strains hereafter denominated as R1 to R3 for cases 1 to 3). The genome of each strain was sequenced and analyzed to confirm that the infection and relapse strains were indeed the same and not a case of re-infection (Table 1). Interestingly, antimicrobial susceptibility testing (Supplementary Table 1) and *in silico* analysis after whole genome sequencing (Supplementary Data 1) did not reveal any acquisition of antibiotic resistance associated with the relapse events. Consequently, each strain pair was examined for other phenotypic and genetic features that could have been selected to allow the infection relapses.

364 Table 1. Cases and strain information. Table summarizing the type and location of infection as well as type of sample. Each strain was typed *in silico* and, when the infection

365 was polymicrobial, the other species involved are listed.

366

Case N°	Strain	Infection status	Infection site	Sample type	Diagnosis	Time before relapse	Antibiotic susceptibility profile	Phylogroup	Serotype	ANI	MLST #1	MLST #2	fimH	fumC	Infection type	Other pathogens if polymicrobial
1	I1	Initial	Hand	Deep tissue by swab	Septic arthritis 4th finger (no material)	51 days	Penicillinase	B1	O76:H28	99.99%	224	730	FimH39	FumC4	Monomicrobial	
	R1	relapse		Deep tissue by swab			Identical								Polymicrobial	*Enterococcus faecium*, *Pseudomonas aeruginosa*, *Citrobacter freundii*
2	I2	Initial	Spine	Washing liquid	Vertebral osteomyelitis (no material)	748 days	ESBL-producing	G	O24:H4	99.99%	117	48	FimH97	FumC45	Monomicrobial	
	R2	relapse		biopsy			Identical								Polymicrobial	*Cutibacterium acnes*
3	I3	Initial	Right hip	Bone	Prosthetic joint infection	66 days	ESBL-producing	A	O89/O162:H9	99.99%	167	2	/	FumC11	Monomicrobial	
	R3	relapse		Deep tissue			Identical								Monomicrobial	

367

368

369

370 The first notable difference identified by genomic analysis was the number of gained
371 and lost genes (Supplementary Table 4), some of which corresponding to potential plasmids
372 (Supplementary Data 2). Particularly, the R2 strain that displayed the longest in-patient
373 evolution underwent an important genome reduction with the loss of 3.4% of its size
374 corresponding to 170 coding sequences involved in various functions such as transport, iron
375 acquisition, carbohydrate acquisition and utilization, defense against competitors with Microcin
376 H47 production-related genes and three adhesins (Supplementary Data 2).

377

378 The number of mutations per base per year was quite high for all three relapse strains ($1.1x10^{-}$
379 ^{6} to $8.4x10^{-6}$) as compared to what was reported in the literature ($6.9x10^{-7}$ for *E. coli* ED1a in
380 the gut, (45)). In addition, even if no functional convergence was observed in the mutated genes,
381 the predominance of loss of function and non-synonymous mutations suggests that positive
382 selection was at play in these cases (Table 2).

383

384 Table 2. SNP analysis in the relapse strains. SNPs, insertions and deletions identified in the evolved strains as compared to their related ancestor.

385

386

Strain	Mutation	Annotation	Impact	Gene	Description
R1	T→A	intergenic (+168/-221)	Intergenic	uidR → / → uidA	transcriptional repressor/beta-D-glucuronidase
	A→G	N16D (AAC→GAC)	Non-synonymous	yehT →	putative response regulator in two-component system withYehU
	T→C	T46A (ACA→GCA)	Non-synonymous	rppH ←	RNA pyrophosphohydrolase
	T→C	K577E (AAG→GAG)	Non-synonymous	ydiJ ←	putative FAD-linked oxidoreductase
R2	G→A	G335G (GGC→GGT)	Synonymous	COMLMOEC_00122 ←	hypothetical protein
	C→G	V16L (GTA→CTA)	Non-synonymous	insK_3 ←	IS150 transposase B
	C→G	S67T (AGC→ACC)	Non-synonymous	COMLMOEC_04582 ←	IS3 family transposase IS629
	C→T	A131T (GCC→ACC)	Non-synonymous	ebgR ←	transcriptional repressor
	C→T	A197V (GCC→GTC)	Non-synonymous	COMLMOEC_04752 →	IS66 family transposase ISEc47
	T→A	I263N (ATT→AAT)	Non-synonymous	btuC →	vitamin B12 ABC transporter permease
	A→G	intergenic (+1283/–)	Intergenic	COMLMOEC_01687 → / –	hypothetical protein/–
	A→C	intergenic (+352/–)	Intergenic	COMLMOEC_04947 → / –	hypothetical protein/–
R3	G→T	E297D (GAG→GAT)	Non-synonymous	hypT →	hypochlorite-responsive transcription factor
	G→A	D119N (GAT→AAT)	Non-synonymous	insF1_1 →	IS3 transposase B
	+G	coding (1001/1041 nt)	Loss of function	vgrG1 →	Actin cross-linking toxin VgrG1
	C→T	intergenic (+315/-76)	Intergenic	uidR → / → uidA	transcriptional repressor/beta-D-glucuronidase
	(GTGGCTGTT)8→10	coding (1850/2208 nt)	Loss of function	traD ←	Coupling protein TraD
	Δ1 bp	intergenic (-142/+229)	Intergenic	araD ← / ← araA	L-ribulose-5-phosphate 4-epimerase/L-arabinose isomerase

387

388

389

390

391

392 **II- *In vivo* adaptation did not modify motility and biofilm formation capacities.**

393

394 Because strain motility could impact virulence, we tested each strain on low-agar LB
395 plates at 30°C and 37°C, which showed that the second and third pairs of strains were non-
396 motile (Supplementary Figure 2). Both I1 and R1 strains display temperature-dependent
397 motility very likely due to a flagellin production restricted to 30°C (Supplementary Figures 2
398 and 3, see Supplementary Results).

399

400 Since biofilm formation is related to bacterial motility and sometimes involved in
401 infection relapses, we analyzed the biofilm-forming capacity of each strain on different
402 surfaces, which showed that the R1 relapse strain formed 1.71 more biofilms than I1 strain
403 when grown on silicon coupons (Figure 1.A). No difference was identified for the I2-R2 pair
404 (Figure 1.B), while the R3 relapse strain had a significant but very low increase in biofilm
405 formation on PVC plates (1.08-fold) (Figure 1.C). This slight increase was reversed when
406 grown on silicone since the I3 strain showed a 1.49 increase in biofilm formation (Figure 1.C).
407 However, in all cases the tested clinical strains showed a weak biofilm-forming capacity, all of
408 them being equivalently or even less efficient than *E. coli* K12 strain MG1655 used as a control
409 for weak biofilm formation. Interestingly, R1 strain showed a slight decrease of its adhesion
410 capacity to osteoblasts (Figure 1.D). However, no evident genetic modification could be linked
411 to this phenotype. No difference was observed either in terms of auto-aggregation or production
412 of curli amyloids and cellulose (Supplementary Figure 4 and Supplementary Results). Taken
413 together, these results suggest that a modification of biofilm formation and biofilm-related
414 phenotypes were unlikely to be involved in *in vivo* adaptation in these three studied cases.

415

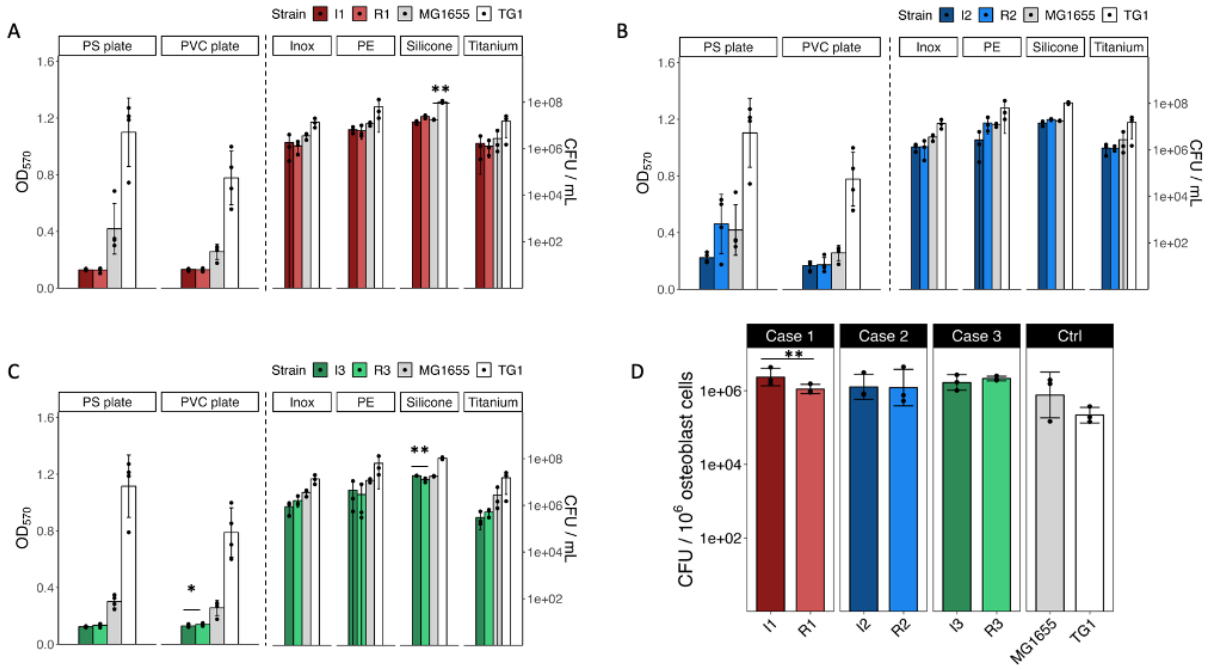

Figure 1. Biofilm formation capacity for infection and relapse strains from cases 1 (**A**), 2 (**B**) and 3 (**C**). Six different surfaces were tested, *E. coli* K12 MG1655 was used as a control for weak biofilm formation and *E. coli* TG1 as a control for strong biofilm formation. Biofilm formation on PS and PVC plates was assessed by crystal violet assay (n=4 biological replicates) and is plotted on left y-axis, while the biofilm formation on the other surfaces was assessed by CFU count (n=3 biological replicates) and are plotted on the right y-axis. (D) Adhesion capacity on osteoblast human cells (n=3 biological replicates). Statistical significance according to non-parametric Mann-Whitney test. * $p<0.05$; ** $p<0.01$.

III- Loss of adhesins induces serum resistance in R2 strain.

To assess the strain capacity to challenge to the host immune defenses, we measured the survival of all strains exposed to active human serum. While we observed no difference between I3 and R3 strains, the relapse strain R1 had a slight decrease in serum resistance compared to I1 strain and the relapse strain R2 had a clear increase in serum resistance relatively to its ancestral strain I2 (Figure 2.A). Although we identified no difference in the I2 *vs* R2 lipopolysaccharide profile (outer-membrane component targeted by the complement) (Figure 2.B), the loss of two adhesins in R2 could be linked to this phenotype (Supplementary Data 2)

435 (11). Indeed, deletion of each adhesin in I2 strain led to reduced serum resistance suggesting
436 that the loss of both adhesins could have been selected through the conferred immune system
437 evasion, contributing to the strain adaptation to the host environment (Figure 2.C).
438 Unfortunately, we were unable to assess the additive effect of these mutations since we could
439 not reconstruct the double mutant in the I2 strain despite repeated attempts.

440

441

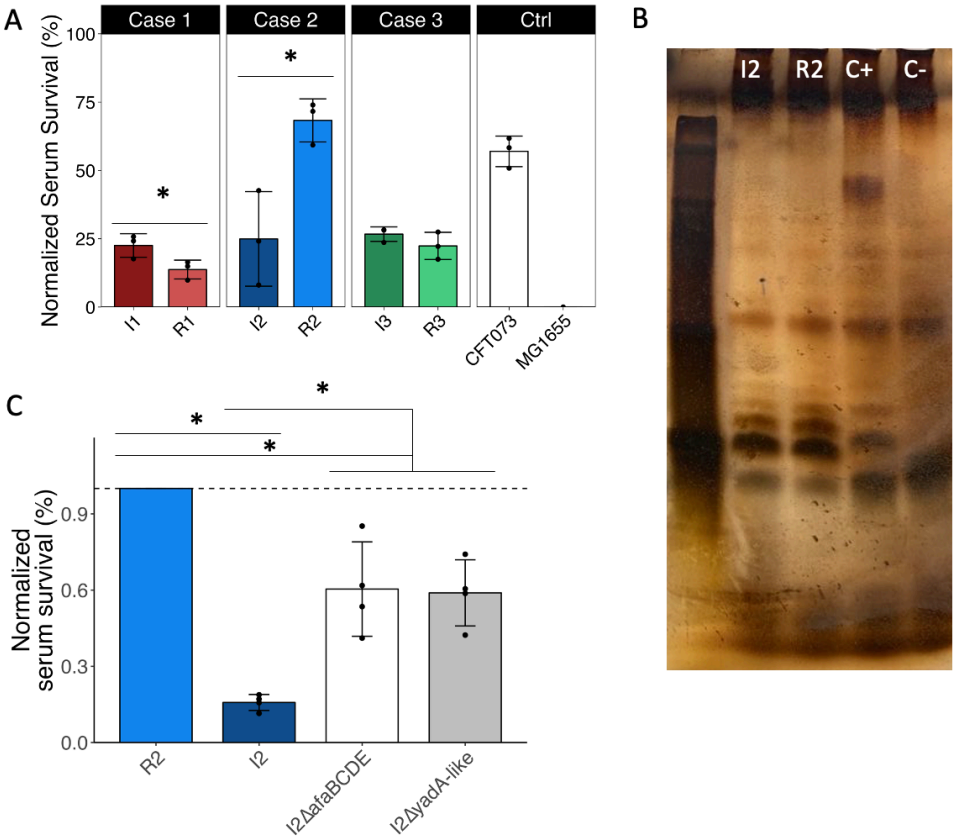

442

443 **Figure 2**. Serum survival capacity. **A**. Normalized serum survival capacity of each strain expressed as percentage
444 of the control for growth in Heat Inactivated Serum (HIS). *E. coli* strains CFT073 and MG1655 were used as
445 positive and negative controls, respectively. **B**. LPS profile of I2 and R2 strains. *E. coli* MG1655 was used as a
446 negative control and the same strain in which the O-Antigen was reconstructed was used as a positive control. **C**.
447 Serum survival of I2 ancestral strain, R2 relapse strain as well as two deletion mutants constructed in the I2
448 ancestral strain: one for the *afa* afimbrial operon and a second for the *yadA*-like encoding gene.

449

450
451
452
453
454 **IV-Strain virulence was not targeted during in-patient selection.**
455
456 To gain insight into the potential evolution of the virulence of the studied strains, we
457 assessed their cytotoxicity on HeLa cells as well as hemolysis capacities and showed no
458 differences, except for a slightly lower hemolysis induced by R2 strain after 24h of incubation
459 in presence of defibrinated horse blood (Figure 3.A.B).
460
461

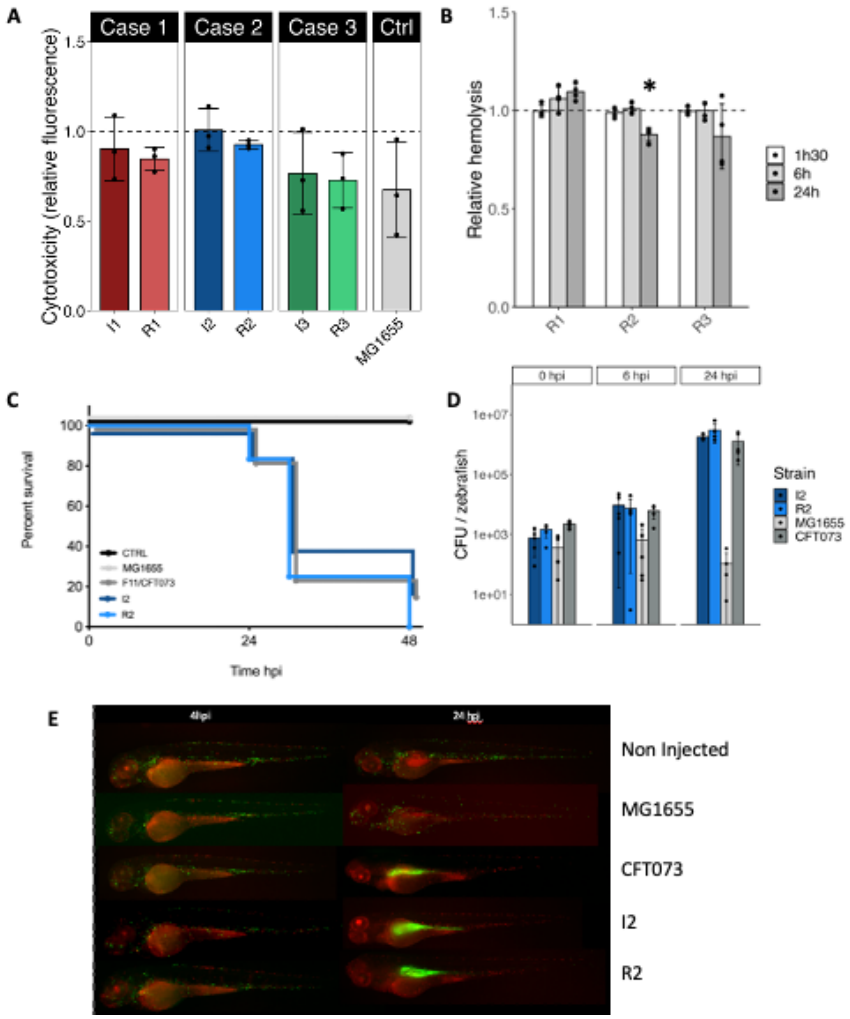

462
463 **Figure 3**. Virulence of the strains. (**A**) Cytotoxicity test on HeLa cells. All six adapted and ancestral strains were
464 tested as well as MG1655 strain as a negative control. The values for each strain were expressed relatively to the

465 control without bacteria. Values are represented as a mean of three biological replicates +/- SD. (**B**) Hemolysis
466 capacity in liquid culture of each relapse strain relatively to its ancestor. Values are represented as a mean of four
467 biological replicates +/- SD. (**C**) Monitoring of zebrafish survival, (**D**) bacterial burden into the zebrafish and (**E**)
468 *in vivo* fluorescence of macrophages and neutrophils for zebrafish infected by I2 and R2 strains as well as non-
469 injected control, MG1655 strain (negative control) and CFT073 (positive control). Each image is representative
470 of 5 biological replicates. Fifteen zebrafish were used for each experiment in C and D.
471
472
473
474 Potential differences in *in vivo* virulence were tested in a zebrafish (*Danio rerio*) larval model
475 (47). While no differences were found in bacterial load for all pairs (Sup Figure S5.A.B.C),
476 zebrafish larvae exposed to R2 relapse strain had a slightly lower survival 24 hours post-
477 infection (hpi) than with its related ancestor I2, even though both strains ultimately induced the
478 same level of mortality 48 hpi (Figure 3.C.D). No difference was identified concerning the
479 zebrafish innate immune response level (Figure 3.E). These results suggest that the R2 relapse
480 strain induced slightly quicker mortality, which does not seem to be linked to a difference in
481 colonization ability.
482

483 V- Growth optimization and colicin production as strategies to outcompete 484 other bacteria.

485
486 To assess if a difference in growth capacity could advantage the strains isolated after
487 relapses, they were pitted against their related ancestor in 1:1 ratio competition experiments in
488 biofilm and liquid conditions. First, no difference in fitness was observed in biofilm condition,
489 which further straightened the hypothesis that biofilm formation was not targeted during the *in*
490 *vivo* adaptation. In liquid, while R1 strain slightly outcompeted its ancestor I1, R2 strain had a
491 striking fitness advantage over I2 (Figure 4.A).

492 To further investigate this phenotype, we competed I2 and R2 strains in presence of
493 different sugars as well as of an iron chelator (2,2'-Bipyridyl) based on identified genetic
494 modifications and especially gene losses related to uptake and metabolism of these substrates
495 (Supplementary Data 2). Surprisingly, despite these gene losses, R2 strain showed no growth
496 defect and even globally had an advantage through a capacity to better sustain growth during
497 the stationary phase (Supplementary Figure 6), as confirmed by competition assays (Figure
498 4.B). Therefore, extensive gene loss seems to have resulted in a global growth optimization,
499 which could have helped the strain to outcompete other bacteria including its ancestor.
500 Another strategy to outcompete its kin and promote subsequent adaptation was
501 identified in the relapse strain R1, which acquired a colicin-producing plasmid allowing the
502 production of colicin E1. An overlay assay indeed confirmed the acquired capacity of R1
503 relapse strain to inhibit I1 strain growth (Supplementary Figure 7).
504
505
506

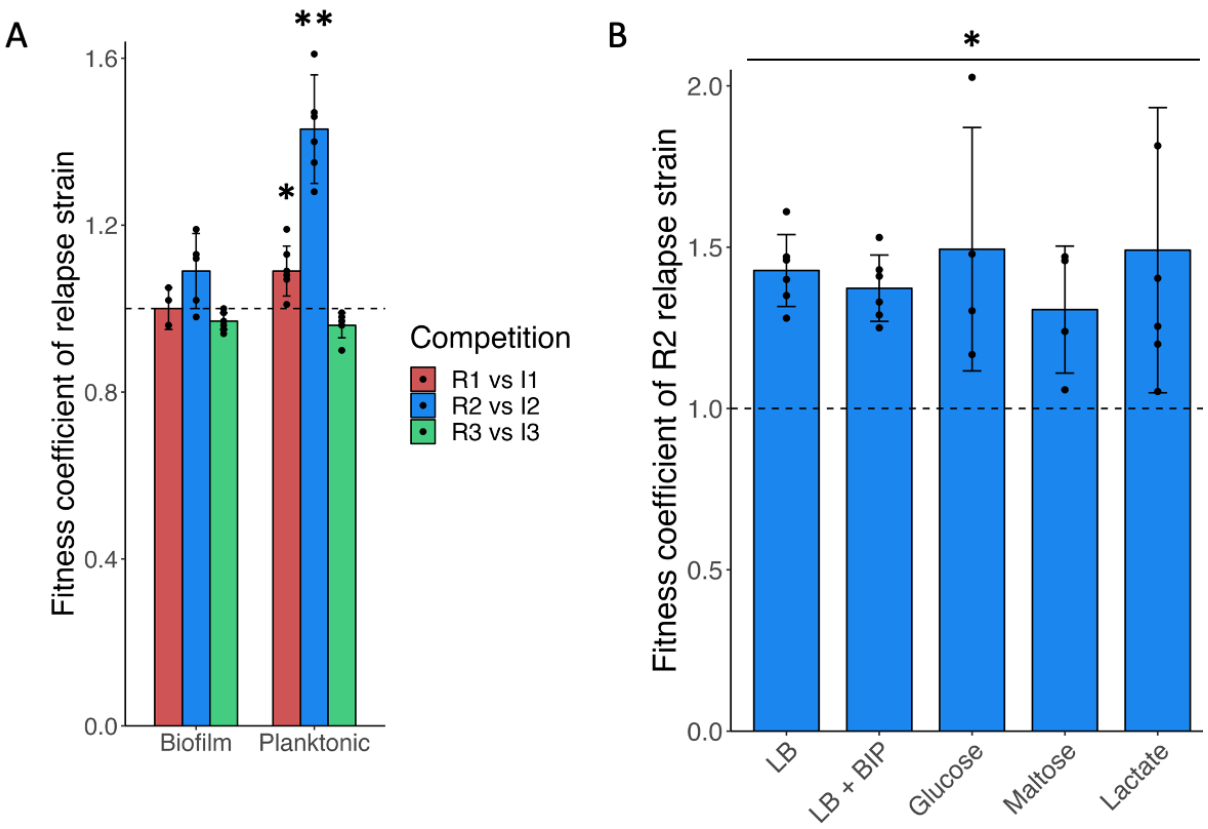

507

508 **Figure 4**. Fitness competitions and growth capacities. (**A**) Fitness competitions of relapse against ancestral strain
509 for all three pairs in planktonic and biofilm conditions. Values are expressed as the mean of six biological replicates
510 +/- SD with statistical significance according to Mann-Whitney test (*: p-value < 0.05, **: p-value < 0.01). **B**.
511 Fitness competitions of R2 relapse strain against I2 ancestral strain in different conditions (same as in
512 supplementary Figure S6.B-F). BIP: 2,2'-Bipyridyl. Values are the mean of four to six biological replicates +/-
513 SD with statistical significance according to Mann-Whitney test (*: p-value < 0.05).

514

515

516 # Discussion (853 words)

517

518 Treatment failure is a common issue of BJIs, allowing bacteria to remain and adapt to
519 the host, ultimately increasing the risk of relapse and the difficulty to cure the patient. A better
520 understanding of the mechanisms underlying pathogens' adaptation to the host environment
521 would allow for improving the management of relapsing BJIs. Here we investigated three cases
522 of BJIs relapse involving pathogenic *E. coli*.
523 Both our genetic and phenotypic analysis highlighted a diversity of functions emerging from
524 bacterial adaptation to the host environment during BJIs. We found that adapted strains isolated
525 from relapses displayed a relatively high mutation rate, which is a known adaptive advantage
526 increasing the probability to produce advantageous mutations that could be subsequently
527 selected (13, 48, 49). However, we did not identify any mutation in genes known to be involved
528 in DNA damage repair, suggesting that these high mutation rates were not acquired during
529 adaptation to the host environment but rather intrinsic to these strains. This, in addition to stress-
530 induced mutagenesis, could have further promoted the selection of beneficial traits, probably
531 partly explaining their adaptive success.
532 Biofilms are known to be frequently involved in infections and relapses, including BJIs.
533 However, none of the three investigated cases showed an increased biofilm formation capacity
534 that could have played a role in the relapses and all strains were even characterized as poor *in*
535 *vitro* biofilm formers. However, these infections were bone- or tissue-related and strong *in vitro*
536 biofilm capacity may not necessarily translate into a selective advantage in this type of
537 infections as compared to prosthesis-related infections, which were shown to be caused by a
538 majority of strong biofilm formers (50). In these cases, the capacity to form biofilm correlate
539 with the severity of the clinical outcome (51–53), while it was not the case for strains isolated
540 from non-orthopedic biofilm infections (54, 55).

541 Another critical selection pressure faced by pathogenic bacteria is the host immune system. The
542 inhibition of the production of flagellin, a known target of immune defenses, at 37°C by I1 and
543 R1 strains, could minimize their recognition in the host environment (56, 57). This could not
544 only contribute to immune system evasion but also to save energy through a down-regulation
545 or suppression of flagellin production, as shown to be the case in the context of gut infection
546 by *E. coli* (58, 59).
547 This immune system evasion strategy is even clearer in the case of the R2 relapse strain, which
548 adapted and showed increased survival to human serum through the loss of two adhesins. The
549 fact that the loss of two virulence factors could confer a selective advantage may suggest that,
550 in these specific cases, virulence could be less important than evading the immune system as
551 shown to happen during *in vivo* adaptation (60, 61), allowing pathogens to stay longer in the
552 host. This trend was illustrated by the infection experiments performed in zebrafish, where no
553 difference was observed at the exception of the R2 strain that induced a slightly higher mortality
554 at 24hpi.
555 In addition, the R2 strain presented an interesting case of gene loss. Whereas genome reduction
556 is usually considered as a strategy by which selection reduces energy consumption via the loss
557 of genes and functions that are not used or under selective pressure (62, 63). In the case of the
558 R2 strain, numerous gene losses seem to result in a global optimization of growth capacities,
559 potentially correlated to lower the cost associated with the production of unnecessary genes and
560 lower amount of DNA to replicate. It is possible that some nutritional resources could be
561 directly acquired from the new host environment instead of being synthesized by the cells and
562 that the loss of genes involved in this production optimizes the cell metabolism (64). Gain of
563 growth rate or capacity in the context of an infection could be of paramount importance to
564 outcompete other endogenous or pathogenic bacteria and thrive in the host environment. Such
565 cases of genome reduction-induced complexification are more and more documented (20, 21)

566 showing that innovation can also rise from gene loss and not only from gene gains or
567 duplications followed by neo- or sub-functionalization (65).
568 Finally, it is an important parameter to stress the polymicrobial context of some of these BJIs
569 infections, in which interactions between the different bacterial species or strains could play an
570 important role in the relapses as well as in the mechanisms shaping bacterial adaptation to the
571 host environment (66, 67). Some key phenomenon involved in the relapse or strain adaptation
572 could therefore be dependent on bacteria-bacteria direct or indirect interactions and
573 consequently missed in this study. However, both the limited number of strains investigated
574 and the fact that all three cases corresponded to different BJIs could also account for the
575 observed differences in strain profile and mechanisms involved in their *in vivo* adaptation.
576 Further investigations with a larger cohort would help determine whether these diverse profiles
577 and adaptive strategies are due to the various types of infection investigated here or if it
578 constitutes a more general rule of *E. coli* pathogenic strain in BJIs. It would also help identify
579 if some adaptive strategies are preferentially selected in relapse cases.
580
581
582 **ACKNOWLEDGEMENTS**
583 This work was supported by the French National Research Agency (ANR), project EvolTolAB
584 (ANR-18-CE13-0010), by the French government's Investissement d'Avenir Program,
585 Laboratoire d'Excellence "Integrative Biology of Emerging Infectious Diseases" (grant
586 n°ANR-10-LABX-62-IBEID) and by the Fondation pour la Recherche Médicale (grant
587 DEQ20180339185). S.T.-R was supported by the French National Research Agency (ANR),
588 project EvolTolAB (ANR-18-CE13-0010).
589 We thank Dr. Emma Colucci-Guyon and Dr. Laurent Boucontet for critical reading of the
590 manuscript. We are grateful to the Zebrafish Projects Hub of the Institut Pasteur and especially

591 to Dr. Emma Colucci-Guyon and Dr. Laurent Boucontet who carried out the infection
592 experiments in zebrafish larvae. We are grateful to Dr. Monica Rolando for kindly providing
593 the anti-flagellin antiserum. We are grateful to Emmanuel Chanard from Cerballiance for
594 providing strains and microbiological information.
595 All authors declare no competing financial interests.

596

597

598

599 # References

600 1. Osmon DR, Berbari EF, Berendt AR, Lew D, Zimmerli W, Steckelberg JM, Rao N,
601 Hanssen A, Wilson WR, Infectious Diseases Society of America. 2013. Diagnosis and
602 management of prosthetic joint infection: clinical practice guidelines by the Infectious
603 Diseases Society of America. Clin Infect Dis 56:e1–e25.
604 2. Tande AJ, Patel R. 2014. Prosthetic joint infection. Clin Microbiol Rev 27:302–345.
605 3. Tong SYC, Davis JS, Eichenberger E, Holland TL, Fowler VG. 2015. Staphylococcus
606 aureus infections: epidemiology, pathophysiology, clinical manifestations, and management.
607 Clin Microbiol Rev 28:603–661.
608 4. Laurent E, Gras G, Druon J, Rosset P, Baron S, Le-Louarn A, Rusch E, Bernard L,
609 Grammatico-Guillon L. 2018. Key features of bone and joint infections following the
610 implementation of reference centers in France. Med Mal Infect 48:256–262.
611 5. Ferguson J, Alexander M, Bruce S, O'Connell M, Beecroft S, McNally M. 2021. A
612 retrospective cohort study comparing clinical outcomes and healthcare resource utilisation in
613 patients undergoing surgery for osteomyelitis in England: a case for reorganising orthopaedic
614 infection services. J Bone Jt Infect 6:151–163.
615 6. Cerioli M, Batailler C, Conrad A, Roux S, Perpoint T, Becker A, Triffault-Fillit C,
616 Lustig S, Fessy M-H, Laurent F, Valour F, Chidiac C, Ferry T. 2020. Pseudomonas
617 aeruginosa Implant-Associated Bone and Joint Infections: Experience in a Regional
618 Reference Center in France. Front Med (Lausanne) 7:513242.
619 7. Triffault-Fillit C, Ferry T, Laurent F, Pradat P, Dupieux C, Conrad A, Becker A,
620 Lustig S, Fessy MH, Chidiac C, Valour F, Lyon BJI Study Group. 2019. Microbiologic
621 epidemiology depending on time to occurrence of prosthetic joint infection: a prospective
622 cohort study. Clin Microbiol Infect 25:353–358.
623 8. Joo H-S, Cheung GYC, Otto M. 2011. Antimicrobial activity of community-
624 associated methicillin-resistant Staphylococcus aureus is caused by phenol-soluble modulin
625 derivatives. J Biol Chem 286:8933–8940.
626 9. Majeed H, Gillor O, Kerr B, Riley MA. 2011. Competitive interactions in Escherichia
627 coli populations: the role of bacteriocins. ISME J 5:71–81.
628 10. Baishya J, Wakeman CA. 2019. Selective pressures during chronic infection drive
629 microbial competition and cooperation. 1. npj Biofilms Microbiomes 5:1–9.
630 11. Klemm P, Roos V, Ulett GC, Svanborg C, Schembri MA. 2006. Molecular

631 characterization of the Escherichia coli asymptomatic bacteriuria strain 83972: the taming of a
632 pathogen. Infect Immun 74:781–785.
633 12. Price EP, Sarovich DS, Mayo M, Tuanyok A, Drees KP, Kaestli M, Beckstrom-
634 Sternberg SM, Babic-Sternberg JS, Kidd TJ, Bell SC, Keim P, Pearson T, Currie BJ. 2013.
635 Within-host evolution of Burkholderia pseudomallei over a twelve-year chronic carriage
636 infection. mBio 4:e00388-13.
637 13. Lieberman TD, Flett KB, Yelin I, Martin TR, McAdam AJ, Priebe GP, Kishony R.
638 2014. Genetic variation of a bacterial pathogen within individuals with cystic fibrosis
639 provides a record of selective pressures. Nat Genet 46:82–87.
640 14. Marvig RL, Johansen HK, Molin S, Jelsbak L. 2013. Genome analysis of a
641 transmissible lineage of pseudomonas aeruginosa reveals pathoadaptive mutations and
642 distinct evolutionary paths of hypermutators. PLoS Genet 9:e1003741.
643 15. Klemm EJ, Gkrania-Klotsas E, Hadfield J, Forbester JL, Harris SR, Hale C, Heath JN,
644 Wileman T, Clare S, Kane L, Goulding D, Otto TD, Kay S, Doffinger R, Cooke FJ,
645 Carmichael A, Lever AML, Parkhill J, MacLennan CA, Kumararatne D, Dougan G, Kingsley
646 RA. 2016. Emergence of host-adapted Salmonella Enteritidis through rapid evolution in an
647 immunocompromised host. 3. Nat Microbiol 1:1–6.
648 16. Feliziani S, Marvig RL, Luján AM, Moyano AJ, Di Rienzo JA, Krogh Johansen H,
649 Molin S, Smania AM. 2014. Coexistence and Within-Host Evolution of Diversified Lineages
650 of Hypermutable Pseudomonas aeruginosa in Long-term Cystic Fibrosis Infections. PLoS
651 Genet 10:e1004651.
652 17. Smith EE, Buckley DG, Wu Z, Saenphimmachak C, Hoffman LR, D'Argenio DA,
653 Miller SI, Ramsey BW, Speert DP, Moskowitz SM, Burns JL, Kaul R, Olson MV. 2006.
654 Genetic adaptation by Pseudomonas aeruginosa to the airways of cystic fibrosis patients. Proc
655 Natl Acad Sci U S A 103:8487–8492.
656 18. Losada L, Ronning CM, DeShazer D, Woods D, Fedorova N, Kim HS, Shabalina SA,
657 Pearson TR, Brinkac L, Tan P, Nandi T, Crabtree J, Badger J, Beckstrom-Sternberg S, Saqib
658 M, Schutzer SE, Keim P, Nierman WC. 2010. Continuing evolution of Burkholderia mallei
659 through genome reduction and large-scale rearrangements. Genome Biol Evol 2:102–116.
660 19. Linz B, Ivanov YV, Preston A, Brinkac L, Parkhill J, Kim M, Harris SR, Goodfield
661 LL, Fry NK, Gorringe AR, Nicholson TL, Register KB, Losada L, Harvill ET. 2016.
662 Acquisition and loss of virulence-associated factors during genome evolution and speciation
663 in three clades of Bordetella species. BMC Genomics 17:767.
664 20. Bolotin E, Hershberg R. 2015. Gene Loss Dominates As a Source of Genetic
665 Variation within Clonal Pathogenic Bacterial Species. Genome Biol Evol 7:2173–2187.
666 21. Albalat R, Cañestro C. 2016. Evolution by gene loss. Nat Rev Genet 17:379–391.
667 22. Trouillet-Assant S, Lelièvre L, Martins-Simões P, Gonzaga L, Tasse J, Valour F,
668 Rasigade J-P, Vandenesch F, Muniz Guedes RL, Ribeiro de Vasconcelos AT, Caillon J,
669 Lustig S, Ferry T, Jacqueline C, Loss de Morais G, Laurent F. 2016. Adaptive processes of
670 Staphylococcus aureus isolates during the progression from acute to chronic bone and joint
671 infections in patients. Cell Microbiol 18:1405–1414.
672 23. Chaveroche MK, Ghigo JM, d'Enfert C. 2000. A rapid method for efficient gene
673 replacement in the filamentous fungus Aspergillus nidulans. Nucleic Acids Res 28:E97.
674 24. Sprouffske K, Wagner A. 2016. Growthcurver: an R package for obtaining
675 interpretable metrics from microbial growth curves. BMC Bioinformatics 17:172.
676 25. Phan QT, Sipka T, Gonzalez C, Levraud J-P, Lutfalla G, Nguyen-Chi M. 2018.
677 Neutrophils use superoxide to control bacterial infection at a distance. PLOS Pathogens
678 14:e1007157.
679 26. Renshaw SA, Loynes CA, Trushell DMI, Elworthy S, Ingham PW, Whyte MKB.
680 2006. A transgenic zebrafish model of neutrophilic inflammation. Blood 108:3976–3978.

681 27. Colucci-Guyon E, Tinevez J-Y, Renshaw SA, Herbomel P. 2011. Strategies of
682 professional phagocytes in vivo: unlike macrophages, neutrophils engulf only surface-
683 associated microbes. J Cell Sci 124:3053–3059.
684 28. Boucontet L, Passoni G, Thiry V, Maggi L, Herbomel P, Levraud J-P, Colucci-Guyon
685 E. 2018. A Model of Superinfection of Virus-Infected Zebrafish Larvae: Increased
686 Susceptibility to Bacteria Associated With Neutrophil Death. Front Immunol 9:1084.
687 29. Mostowy S, Boucontet L, Mazon Moya MJ, Sirianni A, Boudinot P, Hollinshead M,
688 Cossart P, Herbomel P, Levraud J-P, Colucci-Guyon E. 2013. The zebrafish as a new model
689 for the in vivo study of Shigella flexneri interaction with phagocytes and bacterial autophagy.
690 PLoS Pathog 9:e1003588.
691 30. Carr IM, Robinson JI, Dimitriou R, Markham AF, Morgan AW, Bonthron DT. 2009.
692 Inferring relative proportions of DNA variants from sequencing electropherograms.
693 Bioinformatics 25:3244–3250.
694 31. Szczesny M, Beloin C, Ghigo J-M. 2018. Increased Osmolarity in Biofilm Triggers
695 RcsB-Dependent Lipid A Palmitoylation in Escherichia coli. mBio 9:e01415-18.
696 32. Mareuil F, Doppelt-Azeroual O, Ménager H. 2017. A public Galaxy platform at
697 Pasteur used as an execution engine for web services . F1000Research 6.
698 33. Bankevich A, Nurk S, Antipov D, Gurevich AA, Dvorkin M, Kulikov AS, Lesin VM,
699 Nikolenko SI, Pham S, Prjibelski AD, Pyshkin AV, Sirotkin AV, Vyahhi N, Tesler G,
700 Alekseyev MA, Pevzner PA. 2012. SPAdes: a new genome assembly algorithm and its
701 applications to single-cell sequencing. J Comput Biol 19:455–477.
702 34. Seemann T. 2014. Prokka: rapid prokaryotic genome annotation. Bioinformatics
703 30:2068–2069.
704 35. Simão FA, Waterhouse RM, Ioannidis P, Kriventseva EV, Zdobnov EM. 2015.
705 BUSCO: assessing genome assembly and annotation completeness with single-copy
706 orthologs. Bioinformatics 31:3210–3212.
707 36. Bortolaia V, Kaas RS, Ruppe E, Roberts MC, Schwarz S, Cattoir V, Philippon A,
708 Allesoe RL, Rebelo AR, Florensa AF, Fagelhauer L, Chakraborty T, Neumann B, Werner G,
709 Bender JK, Stingl K, Nguyen M, Coppens J, Xavier BB, Malhotra-Kumar S, Westh H,
710 Pinholt M, Anjum MF, Duggett NA, Kempf I, Nykäsenoja S, Olkkola S, Wieczorek K,
711 Amaro A, Clemente L, Mossong J, Losch S, Ragimbeau C, Lund O, Aarestrup FM. 2020.
712 ResFinder 4.0 for predictions of phenotypes from genotypes. J Antimicrob Chemother
713 75:3491–3500.
714 37. Zankari E, Allesøe R, Joensen KG, Cavaco LM, Lund O, Aarestrup FM. 2017.
715 PointFinder: a novel web tool for WGS-based detection of antimicrobial resistance associated
716 with chromosomal point mutations in bacterial pathogens. J Antimicrob Chemother 72:2764–
717 2768.
718 38. Camacho C, Coulouris G, Avagyan V, Ma N, Papadopoulos J, Bealer K, Madden TL.
719 2009. BLAST+: architecture and applications. BMC Bioinformatics 10:421.
720 39. Larsen MV, Cosentino S, Rasmussen S, Friis C, Hasman H, Marvig RL, Jelsbak L,
721 Sicheritz-Pontén T, Ussery DW, Aarestrup FM, Lund O. 2012. Multilocus sequence typing of
722 total-genome-sequenced bacteria. J Clin Microbiol 50:1355–1361.
723 40. Joensen KG, Tetzschner AMM, Iguchi A, Aarestrup FM, Scheutz F. 2015. Rapid and
724 Easy In Silico Serotyping of Escherichia coli Isolates by Use of Whole-Genome Sequencing
725 Data. J Clin Microbiol 53:2410–2426.
726 41. L R, Tb J, F H, M S, V T, E S, N G, R A, Mcf T, O L, H H, Am H. 2018. CHTyper, a
727 Web Tool for Subtyping of Extraintestinal Pathogenic Escherichia coli Based on the fumC
728 and fimH Alleles. Journal of clinical microbiology 56.
729 42. Beghain J, Bridier-Nahmias A, Le Nagard H, Denamur E, Clermont O. 2018.
730 ClermonTyping: an easy-to-use and accurate in silico method for Escherichia genus strain

731 phylotyping. Microb Genom 4:e000192.
732 43. Douarre P-E, Mallet L, Radomski N, Felten A, Mistou M-Y. 2020. Analysis of
733 COMPASS, a New Comprehensive Plasmid Database Revealed Prevalence of Multireplicon
734 and Extensive Diversity of IncF Plasmids. Front Microbiol 11:483.
735 44. Deatherage DE, Barrick JE. 2014. Identification of mutations in laboratory evolved
736 microbes from next-generation sequencing data using breseq. Methods Mol Biol 1151:165–
737 188.
738 45. Ghalayini M, Launay A, Bridier-Nahmias A, Clermont O, Denamur E, Lescat M,
739 Tenaillon O. 2018. Evolution of a Dominant Natural Isolate of Escherichia coli in the Human
740 Gut over the Course of a Year Suggests a Neutral Evolution with Reduced Effective
741 Population Size. Appl Environ Microbiol 84:e02377-17.
742 46. Wickham H. 2009. ggplot2: Elegant Graphics for Data Analysis. Springer, New York,
743 NY. https://link.springer.com/10.1007/978-0-387-98141-3. Retrieved 7 February 2023.
744 47. Wiles TJ, Bower JM, Redd MJ, Mulvey MA. 2009. Use of Zebrafish to Probe the
745 Divergent Virulence Potentials and Toxin Requirements of Extraintestinal Pathogenic
746 Escherichia coli. PLOS Pathogens 5:e1000697.
747 48. Giraud A, Matic I, Tenaillon O, Clara A, Radman M, Fons M, Taddei F. 2001. Costs
748 and benefits of high mutation rates: adaptive evolution of bacteria in the mouse gut. Science
749 291:2606–2608.
750 49. Tenaillon O, Barrick JE, Ribeck N, Deatherage DE, Blanchard JL, Dasgupta A, Wu
751 GC, Wielgoss S, Cruveiller S, Médigue C, Schneider D, Lenski RE. 2016. Tempo and mode
752 of genome evolution in a 50,000-generation experiment. Nature 536:165–170.
753 50. Kawamura H, Nishi J, Imuta N, Tokuda K, Miyanohara H, Hashiguchi T, Zenmyo M,
754 Yamamoto T, Ijiri K, Kawano Y, Komiya S. 2011. Quantitative analysis of biofilm formation
755 of methicillin-resistant Staphylococcus aureus (MRSA) strains from patients with orthopaedic
756 device-related infections. FEMS Immunol Med Microbiol 63:10–15.
757 51. Svensson Malchau K, Tillander J, Zaborowska M, Hoffman M, Lasa I, Thomsen P,
758 Malchau H, Rolfson O, Trobos M. 2021. Biofilm properties in relation to treatment outcome
759 in patients with first-time periprosthetic hip or knee joint infection. J Orthop Translat 30:31–
760 40.
761 52. Sanchez CJ, Mende K, Beckius ML, Akers KS, Romano DR, Wenke JC, Murray CK.
762 2013. Biofilm formation by clinical isolates and the implications in chronic infections. BMC
763 Infect Dis 13:47.
764 53. Post V, Harris LG, Morgenstern M, Mageiros L, Hitchings MD, Méric G, Pascoe B,
765 Sheppard SK, Richards RG, Moriarty TF. 2017. Comparative Genomics Study of
766 Staphylococcus epidermidis Isolates from Orthopedic-Device-Related Infections Correlated
767 with Patient Outcome. J Clin Microbiol 55:3089–3103.
768 54. Cha J-O, Yoo JI, Yoo JS, Chung H-S, Park S-H, Kim HS, Lee YS, Chung GT. 2013.
769 Investigation of Biofilm Formation and its Association with the Molecular and Clinical
770 Characteristics of Methicillin-resistant Staphylococcus aureus. Osong Public Health Res
771 Perspect 4:225–232.
772 55. Guembe M, Alonso B, Lucio J, Pérez-Granda MJ, Cruces R, Sánchez-Carrillo C,
773 Fernández-Cruz A, Bouza E. 2018. Biofilm production is not associated with poor clinical
774 outcome in 485 patients with Staphylococcus aureus bacteraemia. Clin Microbiol Infect
775 24:659.e1-659.e3.
776 56. Smith KD, Andersen-Nissen E, Hayashi F, Strobe K, Bergman MA, Barrett SLR,
777 Cookson BT, Aderem A. 2003. Toll-like receptor 5 recognizes a conserved site on flagellin
778 required for protofilament formation and bacterial motility. Nat Immunol 4:1247–1253.
779 57. Bambou J-C, Giraud A, Menard S, Begue B, Rakotobe S, Heyman M, Taddei F, Cerf-
780 Bensussan N, Gaboriau-Routhiau V. 2004. In vitro and ex vivo activation of the TLR5

781 signaling pathway in intestinal epithelial cells by a commensal Escherichia coli strain. J Biol
782 Chem 279:42984–42992.
783 58. Giraud A, Arous S, De Paepe M, Gaboriau-Routhiau V, Bambou J-C, Rakotobe S,
784 Lindner AB, Taddei F, Cerf-Bensussan N. 2008. Dissecting the genetic components of
785 adaptation of Escherichia coli to the mouse gut. PLoS Genet 4:e2.
786 59. Leatham MP, Stevenson SJ, Gauger EJ, Krogfelt KA, Lins JJ, Haddock TL, Autieri
787 SM, Conway T, Cohen PS. 2005. Mouse intestine selects nonmotile flhDC mutants of
788 Escherichia coli MG1655 with increased colonizing ability and better utilization of carbon
789 sources. Infect Immun 73:8039–8049.
790 60. Winstanley C, O'Brien S, Brockhurst MA. 2016. Pseudomonas aeruginosa
791 Evolutionary Adaptation and Diversification in Cystic Fibrosis Chronic Lung Infections.
792 Trends Microbiol 24:327–337.
793 61. Viberg LT, Sarovich DS, Kidd TJ, Geake JB, Bell SC, Currie BJ, Price EP. 2017.
794 Within-Host Evolution of Burkholderia pseudomallei during Chronic Infection of Seven
795 Australasian Cystic Fibrosis Patients. mBio 8:e00356-17.
796 62. Moran NA. 2002. Microbial minimalism: genome reduction in bacterial pathogens.
797 Cell 108:583–586.
798 63. Weinert LA, Welch JJ. 2017. Why Might Bacterial Pathogens Have Small Genomes?
799 Trends Ecol Evol 32:936–947.
800 64. D'Souza G, Kost C. 2016. Experimental Evolution of Metabolic Dependency in
801 Bacteria. PLoS Genet 12:e1006364.
802 65. Massingham T, Davies LJ, Liò P. 2001. Analysing gene function after duplication.
803 Bioessays 23:873–876.
804 66. Tay WH, Chong KKL, Kline KA. 2016. Polymicrobial-Host Interactions during
805 Infection. J Mol Biol 428:3355–3371.
806 67. Boldock E, Surewaard BGJ, Shamarina D, Na M, Fei Y, Ali A, Williams A, Pollitt
807 EJG, Szkuta P, Morris P, Prajsnar TK, McCoy KD, Jin T, Dockrell DH, van Strijp JAG,
808 Kubes P, Renshaw SA, Foster SJ. 2018. Human skin commensals augment Staphylococcus
809 aureus pathogenesis. Nat Microbiol 3:881–890.

810

811

812